Magnetised Particle Dynamics in the Presence of Gravitational Waves *

L. Vlahos †

Aristotle University of Thessaloniki,

Department of Physics, Section of Astrophysics, Astronomy and Mechanics,

Thessaloniki, 54124 Greece

Abstract

The non-linear interaction of a strong Gravitational Wave with the plasma during the collapse of a massive magnetized star to form a black hole, or during the merging of neutron star binaries (central engine) was investigated. Under certain conditions this coupling may result in an efficient energy space diffusion of particles. Superposition of many such short lived accelerators, embedded inside a turbulent plasma, may be the source for the observed impulsive short lived bursts. In several astrophysical events, gravitational pulses may accelerate the tail of the ambient plasma to very high energies and become the driver for many types of astrophysical bursts.

Key-words: gravitational waves–compact objects:— particle acceleration.

1. Introduction

The interaction of Gravitational Waves (GW) with the plasma and/or the electromagnetic waves propagating inside the plasma, has been studied extensively (DeWitt & Breme (1960); Cooperstock (1968); Zeĺdovich (1974); Gerlach (1974); Grishchuk & Polnarev (1980); Denisov (1978); Macdonald & Thorne (1982); Demianski (1985); Daniel & Tajima (1997); Brodin & Marklund (1999); Marklund, Brodin & Dunsby (2000); Brodin, Marklund & Dunsby (2000); Brodin, Marklund & Servin (2001); Servin et al. (2000); Servin, Brodin & Marklund (2001); Moortgat & Kuijpers (2003), Vlahos et al. (2004); Voyatzis et al. (2006)). All well known approaches for the study of the wave-plasma interaction have been used, namely the Vlasov-Maxwell equations (Macedo & Nelson (1982)), the MHD equations (Papadopoulos & Esposito (1981); Papadopoulos et al. (2001); Moortgat & Kuijpers (2003)) and the non-linear evolution of charged particles interacting with a monochromatic GW

*Presented at the *Workshop on Cosmology and Gravitational Physics Thessaloniki, December 15-16, 2005, Editor : N. K. Spyrou.*

†In colaboration with G. Voyatzis and D. Papadopoulos

(Varvoglis & Papadopoulos (1992)). The Vlasov-Maxwell equations and the MHD equations were mainly used to investigate the linear coupling of the GW with the normal modes of the ambient plasma, but the normal mode analysis is a valid approximation only when the GW is relatively weak and the orbits of the charged particles are assumed to remain close to the undisturbed ones. Several studies have also explored, using the weak turbulence theory, the non-linear wave-wave interaction of plasma waves with the GW (see Brodin et al. (2000)).

The strong nonlinear coupling of isolated charged particles with a coherent GW was studied using the Hamiltonian formalism (Varvoglis & Papadopoulos (1992); Kleidis, Varvoglis & Papadopoulos (1993); Kleidis et al. (1995)). The main conclusion of these studies was that the coupling between GW and an isolated charged particle gyrating inside a constant magnetic field can be very strong only if the GW is very intense. This type of analysis can treat the full non-linear coupling of the charged particle with the GW but looses all the collective phenomena associated with the excitation of waves inside the plasma and the back reaction of the plasma onto the GW.

Vlahos et al. (2004) re-investigate the non-linear interaction of an electron with a GW inside a magnetic field, using the Hamiltonian formalism. Their study is applicable at the neighborhood of the central engine (collapsing massive magnetic star, see Fryer, Holz & Hughes (2002); Dimmelmeier, Font & Muller (2002); Baumgarte & Shapiro (2003)) or during the final stages of the merging of neutron star binaries (Ruffert & Janka (1998); Shibata & Uryu (2002)). A strong but low frequency (10 KHz) GW can resonate with ambient electrons only in the neighborhood of magnetic neutral sheets and accelerates them to very high energies in milliseconds. Relativistic electrons travel along the magnetic field, escaping from the neutral sheet to the super strong magnetic field, and emitting synchrotron radiation. Vlahos et al. (2004) propose that the passage of a GW through numerous localized neutral sheets will create spiky sources which collectively produce the highly variable in time.

2. The Hamiltonian formulation of the GW-particle interaction

The motion of a charged particle in a curved space and in the presence of a magnetic field is described by a Hamiltonian, which, in a system of units $m = c = G = 1$, is given by

$$H(x^\alpha, p_\alpha) = \frac{1}{2} g^{\mu\nu}(p_\mu - eA_\mu)(p_\nu - eA_\nu) = \frac{1}{2}, \quad \alpha, \mu, \nu = 0, ..., 3. \tag{1}$$

$g^{\mu\nu} = g^{\mu\nu}(x^\alpha)$ are the contravariant components of the metric tensor of the curved space and $A_\mu = A_\mu(x^\alpha)$ are the components of the vector potential of the magnetic field (Misner, Thorne & Wheeler (1973)). The variables p_α are the generalized momenta corresponding to the coordinates x^α, and their evolution with respect to the proper time τ is given by the canonical equations

$$\frac{dx^\alpha}{d\tau} = \frac{\partial H}{\partial p_\alpha}, \quad \frac{dp_\alpha}{d\tau} = -\frac{\partial H}{\partial x^\alpha}. \tag{2}$$

A constant magnetic field $\vec{B} = B_0 \vec{e}_z$ is assumed and is produced by the vector potential

$$A_0 = A_1 = A_3 = 0,\ A_2 = B_0(x^1 + c_0),\ c_0 : \text{const.}, \tag{3}$$

and that a GW propagates in a direction $\vec{k}$ of angle θ with respect to the direction of the magnetic field. In that case the nonzero components of the metric tensor are (see Ohanian (1976); Papadopoulos & Esposito 1981) $g^{00} = 1$ and

$$\begin{array}{ll} g^{11} = \frac{1 - a\sin^2\theta\cos\psi}{-1 + a\cos\psi} & g^{22} = \frac{-1}{1 + a\cos\psi} \\ g^{33} = \frac{1 - a\cos^2\theta\cos\psi}{-1 + a\cos\psi} & g^{13} = g^{31} = \frac{(-a/2)\sin 2\theta\cos\psi}{-1 + a\cos\psi}, \end{array} \tag{4}$$

where a is the amplitude of the GW and $\psi = k_\mu x^\mu = \nu(\sin\theta x^1 + \cos\theta x^3 - x^0)$. The parameter ν is the relative frequency of the GW, i.e. $\nu = \omega/\Omega$, where $\Omega = eB_0/mc$ is the Larmor angular frequency. The scaling $eB_0 = 1$, thus $\Omega = 1$ is used.

In the above formalism, the coordinate x^2 is ignorable, so $p_2 = const.$. By setting the constant c_0 in Eq. (3) equal to p_2 we get an appropriate gauge that reduces by one degree of freedom the Hamiltonian (Eq. (1)), which takes the form

$$H = \frac{1}{2}\left(p_0^2 - \frac{1 - as_\theta^2\cos\psi}{1 - a\cos\psi}p_1^2 - \frac{1 - ac_\theta^2\cos\psi}{1 - a\cos\psi}p_3^2 + \frac{2\alpha s_\theta c_\theta\cos\psi}{1 - a\cos\psi}p_1 p_3 - \frac{x_1^2}{1 + a\cos\psi}\right), \tag{5}$$

where we use the notation $c_\theta = \cos\theta$ and $s_\theta = \sin\theta$ for brevity. The canonical transformation of variables $(x^0, x^1, x^3, p_0, p_1, p_3) \to (\chi, q, \phi, I, p, J)$ is applied and the generating function used is

$$F(x^0, x^1, x^3, I, p, J) = x^0 I + x^1 p + \nu(s_\theta x^1 + c_\theta x^3 - x^0)J.. \tag{6}$$

The relation between the old and the new variables is given by the equations

$$\begin{array}{ll} \chi = x^0, & I = p_0 + p_3/c_\theta \\ q = x^1, & p = p_1 - (s_\theta/c_\theta)p_3 \\ \phi = \nu(s_\theta x^1 + c_\theta x^3 - x^0) & J = p_3/(c_\theta s_\theta). \end{array} \tag{7}$$

In the new variables the Hamiltonian (Eq. (5)) takes the form

$$H = \frac{1}{2}\left(I^2 - 2I\nu J - 2s_\theta\nu Jp - \frac{1 - as_\theta^2\cos\phi}{1 - a\cos\phi}p^2 - \frac{q^2}{1 + a\cos\phi}\right). \tag{8}$$

Since the variable χ is ignorable, I is a constant of motion and Eq. (8) can be studied as a system of two degrees of freedom, where I is a parameter. The variables q and p are associated with the gyro-motion. H is of mod(2π) with respect to the angle-variable ϕ and the variable J is related linearly with the energy $\gamma = (1 - \upsilon^2)^{-1/2}$ of the particles according to the equation

$$\gamma = I - \nu J. \tag{9}$$

The equations of motion are

$$\begin{array}{ll} \dot{q} = -s_\theta\nu J - \frac{1 - as_\theta^2\cos\phi}{1 - a\cos\phi}p & \dot{p} = \frac{q}{1 + a\cos\phi} \\ \dot{\phi} = -\nu I - s_\theta\nu p & \dot{J} = \frac{a}{2}\left(\frac{q^2}{(1 + a\cos\phi)^2} - \frac{c_\theta^2 p^2}{(1 - a\cos\phi)^2}\right)\sin\phi, \end{array} \tag{10}$$

where the dot means derivative with respect to the proper time τ. Furthermore, Eq.(8) can be written as a perturbed Hamiltonian in the usual way, i.e.

$$H = H_0 + aH_1 + a^2 H_2 + ..., \tag{11}$$

where

$$H_m = -(c_\theta^2 p^2 + (-1)^m q^2) \cos^m \phi, \ \ m \geq 1 \tag{12}$$

are the perturbation terms and

$$H_0 = \frac{1}{2}(I^2 - 2I\nu J - 2s_\theta \nu J p) - \frac{1}{2}(p^2 + q^2) \tag{13}$$

is the integrable part of the system that describes the unperturbed helical motion of the particle in the flat space. Considering action-angle variables $(J_1, J_2, \phi_1, \phi_2)$, Eq.(13) takes the form

$$H_0(J_1, J_2) = \frac{I}{2} - I\nu J_1 + \frac{s_\theta^2 \nu^2}{2} J_1^2 - J_2, \tag{14}$$

where $\phi_1 = \phi$, $J_1 = J$ and

$$J_2 = \frac{1}{2\pi} \oint p dq = \frac{1}{2}(I^2 - 2I\nu J + s_\theta^2 \nu^2 J^2 - 1)\ , \ \ \phi_2 = \arcsin\left(\frac{\pm q}{\sqrt{2J_2}}\right).$$

Therefore, the unperturbed system is isoenergeticaly non-degenerate for $\theta \neq 0$ (Arnol'd, Kozlov & Neishtadt (1987)) and the gyro motion of the particles is represented by trajectories that twist invariant tori with angular frequencies $\omega_1 = \partial H_0 / \partial J_1$ and $\omega_2 = \partial H_0 / \partial J_2$. The periodic or quasi-periodic evolution of the trajectories depends on whether the rotation number, defined by

$$\rho = \frac{\omega_1}{\omega_2} = \nu I - s_\theta^2 \nu^2 J_1 = \nu(c_\theta^2 I + s_\theta^2 \gamma), \tag{15}$$

is rational or irrational, respectively.

Most of the invariant tori will persist with the presence of the perturbation introduced by the GW, if the amplitude is suficiently small, according to the KAM theorem (Arnol'd et al. (1987)). The orbits of the particles remain close to the unperturbed ones but their projection on the $x^1 - x^2$ plane is not exactly circular and periodic. Close to the resonant tori, where ρ is rational, the Poincaré-Birkhoff theorem applies; a finite number of pairs of stable and unstable periodic trajectories survive, producing locally a pendulum like topology in phase space (Sagdeev, Usikov & Zaslavsky (1988)).

Since the system is of two degrees of freedom, we can study its evolution by using the Poincaré sections $P_S = \{(\phi, \gamma), q = 0, H = 1/2\}$ choosing specific sets of the parameters a, I, ν and θ. In the numerical calculations, which will follow, we set $I = 1$. For the unperturbed system ($a = 0$) the sections show invariant curves γ =const. For $a \neq 0$ some typical examples are shown in Fig.1.

For small values of a (Fig.1a), the invariant curves are perturbed slightly and only close to the most significant resonances their deformation becomes noticeable.

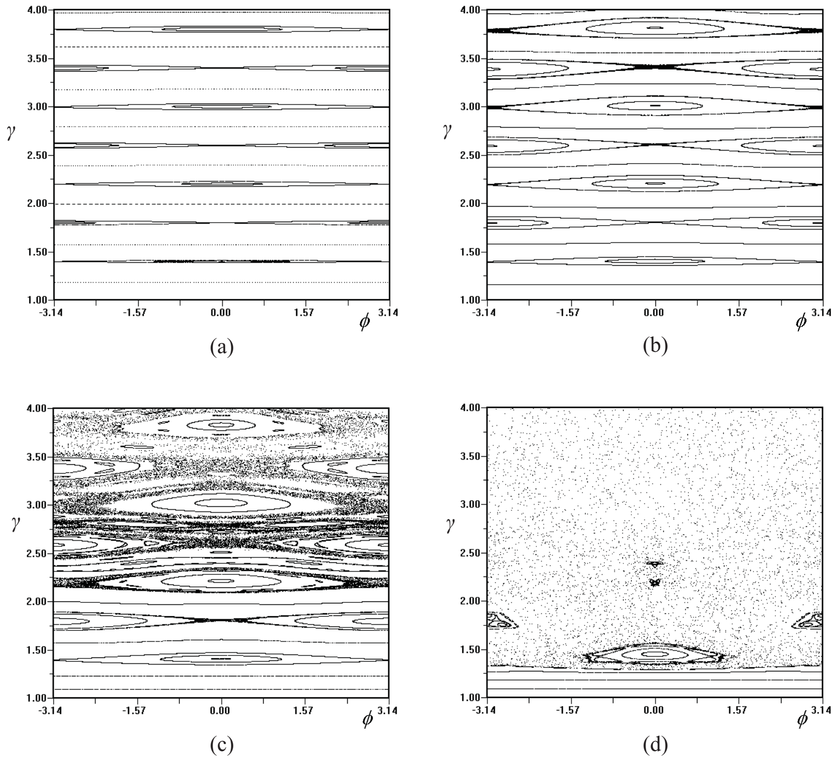

Figure 1: Typical Poincaré sections on the plane (ϕ, γ) of the perturbed system for $\nu = 5, \theta = 45^o$ and a) $a = 0.001$ b) $a = 0.01$ c) $a = 0.02$ and d) $a = 0.1$.

Increasing further the perturbation parameter a, the width of the resonances increases and homoclinic chaos becomes more obvious close to the hyperbolic fixed points (Fig.1b). The existence of invariant curves, which confine the resonant regions, guarantees the bounded variation of the particle's energy ($\Delta\gamma = O(\sqrt{a})$) for the chaotic trajectories.

When the amplitude a exceeds a critical value a_c, overlapping of resonances takes place and large chaotic regions are generated (Fig.1c) (see also Chirikov (1979)). Particles with initial energy γ greater than a critical value γ_c may follow a chaotic orbit which diffuse to regions of higher energy, and this will lead them to very high energies in short time scales. For relatively large values of $\alpha_c << \alpha < 1$, the islands of regular motion, which survive from the resonance overlapping, are gradually destroyed and chaos extends down to relatively low energy particles (Fig.1d). The chaotic part of the phase space will be called "the chaotic sea".

The dynamics, presented by the Poincare sections in Fig.1, is typical for the majority of parameter values. Generally, the critical values a_c and γ_c determine the conditions for possible chaotic diffusion. The dynamics of the charged particles shows some exceptional characteristics when the frequency of the GW is comparable to the Larmor frequency of the unperturbed motion, particularly when $1 \leq \nu < 3$. For such parameter values, stochastic behavior will appear when $\gamma = 1$ and for sufficiently large perturbation values large chaotic regions are generated and diffusion, even for particles with very low initial energies, will be possible. An

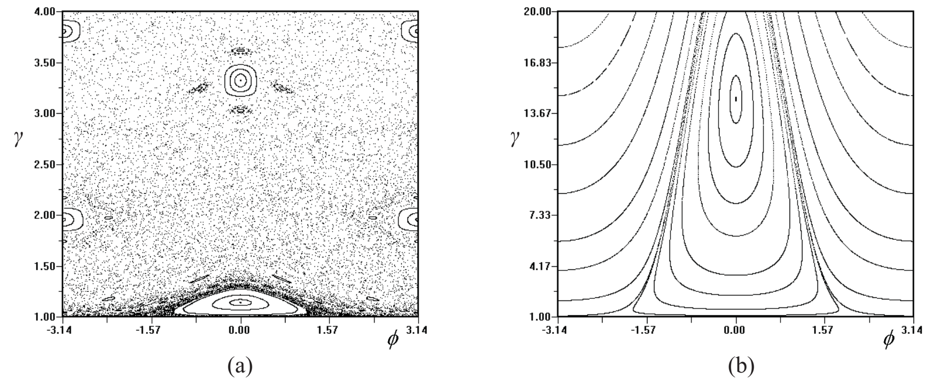

Figure 2: Poincaré sections on the plane (ϕ, γ) a) $a = 0.2, \nu = 2, \theta = 45^o$ b)$a = 0.2, \nu = 1, \theta = 5^o$.

example is shown in Fig.2a.

The evolution of the particles changes character when the direction of propagation of the GW is almost parallel to $\vec{B}$. In this case, chaos disappears, and the particles undergo large energy oscillations. As it is shown in Fig. 2b, a particle, starting even from rest ($\gamma \approx 1$), will be driven regularly to high energies ($\gamma > 20$) and returns back to its initial energy in an almost periodic way. In a realistic, non infinite system, several particles may escape from the interaction with the GW before returning back to low energies. At $\theta = 0$ the system is integrable and the energy of the particles shows regular slow oscillations with an amplitude proportional to a (see Voyatzis et al. (2006) for details).

3. Chaotic diffusion and particle acceleration

In the previous section, we showed that chaotic diffusion is possible for $a \geq a_c$ and for the particles with $\gamma \geq \gamma_c$. Such conditions are necessary but not sufficient for acceleration, since islands of regular motion may be present inside the wide chaotic region (see for example Fig. 2).

In Fig. 3a the evolution of γ along a temporarily trapped chaotic orbit ($\gamma < \gamma_c$) and an orbit which undergoes fast diffusion is shown, using $a = 0.02$. In Fig. 3b we plot the orbit of a particle which on the average is not gaining energy and the average rate of energy gain of 200 particles. The diffusion rate of the particles in the energy space is initially fast but for time $t > 5000$ it starts to slow down. The time t is normalized with the gyro period $2\pi/\Omega$ We study next the evolution of an energy distribution $N(\gamma, t = 0)$ of electrons interacting with the GW. In Fig. 4a we follow the evolution of 3×10^4 particles forming initially a cold energy distribution $N(\gamma, t = 0) \sim \delta(\gamma - 3)$, where δ is the Dirac delta function i.e. all particles have the same initial energy $\gamma = 3$. A large spread in their energy is achieved in short time scales, and for $t = 1000$, a non-thermal tail extending up to $\gamma = 100$ is formed.

We repeat the same analysis, assuming that the initial distribution is the tail ($v > V_{the}$, where V_{the} is the ambient thermal velocity) of a Maxwellian distribution

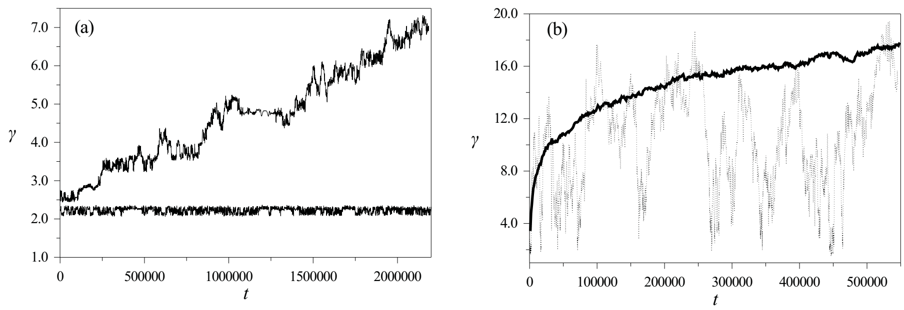

Figure 3: a) The evolution of γ along a trapped in a magnetic island chaotic orbit for $\gamma(0) = 2.2$,$\phi(0) = \pi$ and along a diffusive one for $\gamma(0) = 2.6$, $\phi(0) = 0$ ($a = 0.02, \theta = 45^o, \nu = 5$) b) The evolution of γ along a strongly chaotic orbit (dotted line) and its average value (solid line) along 200 trajectories starting with $\gamma(0) = 2.0$ and a randomly selected $\phi(0)$ ($a = 0.1, \theta = 45^o, \nu = 5$). The time is normalized with the gyro-period ($2\pi/\Omega$).

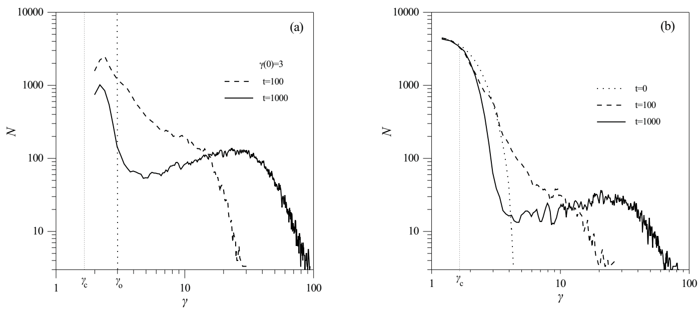

Figure 4: The evolution of an energy distribution. a) The initial distribution (dotted line) consists of 3×10^4 particles having $\gamma(t = 0) = 3$. b) The initial distributions is Maxwellian, as it is shown by the dotted curve. Only particles in the tail of the Maxwellian with $\gamma > \gamma_c$ will be accelerated. The parameters used in both studies are $a = 0.5$, $\nu = 20$ and $\theta = 30^o$.

(Fig.4b). The distribution of the high energy particle form a long non-thermal tail analogously to the results reported in Fig.(4a).

The mean energy diffusion as a function of time is plotted in Fig. **??**a for a particular set of parameters, and it has the general form

$$< \gamma > \sim t^d. \tag{16}$$

From a large number of calculations, we find that the energy spread in time follow a normal diffusion ($d = 0.5$) in energy space but as α increases (see Fig. **??**b), the interaction becomes super-diffusive ($d \geq 0.5$) in energy space. This allows electrons to spread fast in energy space and explains the efficient coupling between the GW and the plasma.

4. Discussion and Summary

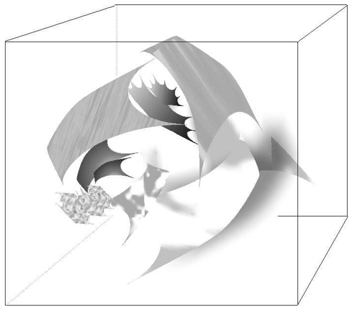

Figure 5: A schematic representation of the thin three dimensional magnetic null sheets appearing spontaneously and fill densely a driven turbulent magnetized plasma

Vlahos et al. (2005) propose a new mechanism for efficient particle acceleration around strong and impulsive sources of GW using the estimates presented above for the strong interaction of GW with electrons. They assume that in the atmosphere of the central engine a turbulent magnetic field will be formed. Inside this complex magnetic topology, a distribution of 3-D magnetic neutral sheets (magnetic null surfaces) (see Fig. 5)

The GW passing through magnetic neutral sheets and claim that the GW will enhance dramatically the acceleration process inside the neutral sheet, causing very intense bursts. We can now list several characteristics of the bursty emission driven by the model proposed above:

- A fraction of the energy carried by the orbital energy of the neutron stars at merger will go to the the GW and a portion of this energy will be transferred to the high energy electrons.
- The topology of the magnetic field varies from event to event, so every burst has its own characteristics.
- The superposition of many small scale localized sources produces a fine time structure on the burst.
- The superposition of null surfaces with a power law distribution of the acceleration lengths will result in a power law energy distribution for the accelerated electrons and an associated synchrotron radiation emitted by the relativistic electrons.
- The decay of the amplitude of the GW and/or the lack of magnetic neutral sheets away from the central engine will mark the end of the burst, but not necessarily the end of other types of bursts since the cooling of the ambient turbulent plasma has a much longer time scale.

On the basis of these findings, we propose that pulsed GW emitted from the central engine will interact with the ambient plasma in the vicinity of the magnetic

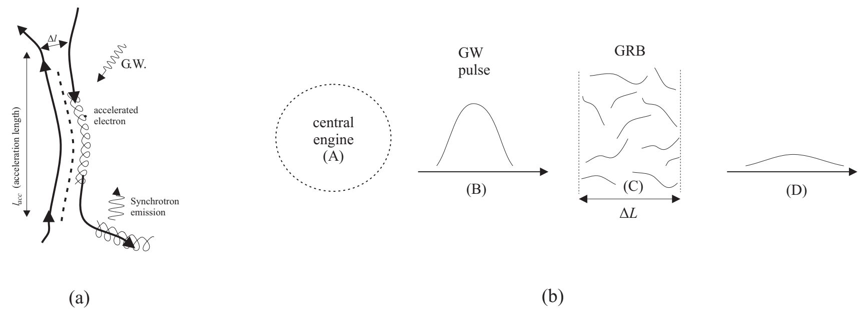

Figure 6: (a) The propagation of a GW through a magnetic neutral sheet accelerates electrons very efficiently. Relativistic electrons stream away from the accelerator and emit a pulse of synchrotron radiation when they reach the super strong magnetic fields. The dashed line represents the magnetic field null surface and ℓ_{acc} is the acceleration length. (b) A collection of magnetic neutral sheets is formed inside the turbulent atmosphere (region C) of the central engine (region A). A GW pulse propagating away from the central engine and passing through the region C will form numerous γ-ray spikes by accelerating particles near the magnetic null surfaces. The superposition of these spikes form a short lived burst. The total burst duration is approximately 100s ($\Delta T \sim \Delta L/c$) but it is composed by many short spikes lasting less than a second (ℓ/c). The GW pulse will become very weak and the density of the magnetic null surfaces will drop dramatically in the region D, and this will mark the end of the burst.

neutral sheets formed naturally inside externally driven turbulent MHD plasmas. Magnetic neutral sheets have characteristic lengths $\ell \sim 10^7 - 10^8$ cm and are short lived 3-D surfaces. Although these structures are efficient accelerators, we are emphasizing in this article only the role of the GW passing through these surfaces since we focus our attention on the very strong and bursty sources. The GW passing through the neutral sheets will accelerate electrons to very high energies (see Fig. 6). Relativistic electrons escape from the magnetic neutral sheets radiating synchrotron emission as soon as they reach the very strong magnetic fields.

A detailed model for the interaction of GW with turbulent MHD plasma is currently under study, and we hope to develop an even more efficient energy transfer from the GW to the plasma e.g by triggering the interaction (percolation) of many null sheets during the passage of the GW. We hope that this may lead us to an alternative scenario for the still unresolved questions related with the acceleration mechanism in the atmosphere of the central engines and the physical processes behind the X-ray and GRB.

Acknowledgements.
This research has been supported in part by a grant (PYTHAGORAS I) from the Ministry of Education of Greece.

References

Arnol'd, V. I., Kozlov V. V., & Neishtadt, A. I., 1987, in Dynamical Systems III, ed. V. I. Arnol'd (Berlin: Springer), 116

Baumgarte, T. W., & Shapiro, S. L., 2003, ApJ, 585, 930

Brodin, G., & Marklund, M., 1999, Phys. Rev. Lett., 82, 3012

Brodin, G., Marklund, M., & Dunsby, P. K. S., 2000, Phys. Rev. D, 62, 104008

Brodin, G., Marklund, M., & Servin, M., 2001, Phys. Rev. D, 63, 124003

Chirikov, B. V., 1979, Phys. Rep. 52, 264

Cooperstock, F. I., 1968, Ann. Phys., 47, 173

Daniel, J., & Tajima, T., 1997), Phys. Rev. D, 55, 5193

Demianski, M., 1985, Relativistic Astrophysics (Oxford: Pergamon)

Denisov, V. I., 1978, Soviet. Phys.-JETP, 42,209

DeWitt, B. S., & Breheme, R. W., 1960, Ann. Physics, 9, 220

Dimmelmeier, H., Font, A. J., & Muller, E., 2002, A&A, 393, 523

Fryer, C. L., Holz, D. E., & Hughes, S. T., 2002, ApJ, 565, 430

Gerlach, U. H., 1974, Phys. Rev. Lett. 32, 1023

Grishchuk, L. P., & Polnarev, A. G., 1980, in General Relativity and Gravitation: One Hundred Years after the Birth of Einstein, Vol. 2, ed. A. Held (New York: Plenum Press), 393

Kleidis, K., Varvoglis, H., & Papadopoulos, D., 1993, A&A, 275, 309

Kleidis, K., et al., 1995, A&A, 294, 313

Macdonald, D., & Thorne, K. S., 1982, MNRAS, 198, 345

Macedo, P. G., & Nelson, A. G., 1982, Phys. Rev. D, 28, 2382

Marklund, M., Brodin, G., & Dunsby, P. K. S., 2000, ApJ, 536, 875

Misner, C. W., Thorne, K. S., & Wheeler, J. A., 1973, Gravitation (San Francisco: Freeman)

Moortgat, J., & Kuijpers, J., 2003, A&A, 402, 905

Ohanian, H. C., 1976, Gravitation and Spacetime (New York: Norton)

Papadopoulos, D., & Esposito, F., 1981, pJ, 248, 783

Papadopoulos, D., et al., 2001), A&A, 377, 701

Ruffert, M., & Janka, H. T., 1998, A&A, 338, 535

Sagdeev, R. Z., Usikov, D. A., & Zaslavsky, G. M., 1988, Nonlinear Physics (New York: Harwood)

Servin, M., et al., 2000, Phys. Rev. E, 62, 8493

Servin, M., Brodin, G., & Marklund, M., 2001, Phys. Rev. D, 64, 024013

Shibata, M., & Uryu, K., 2002, Prog. Theor. Phys., 107, 265

Varvoglis, H., & Papadopoulos, D., 1992, A&A 261, 664

Vlahos, L., Voyatzis, G., & Papadopoulos, D., 2004, ApJ, 604, 297

Voyatzis, G.; Vlahos, L.; Ichtiaroglou, S. & Papadopoulos, D., 2006, Physics Lett. A, 352, 261.

Zeldóvich, Y. B., 1974, Soviet. Phys.-JETP, 38, 652